

# Lawrence Berkeley National Laboratory

## Lawrence Berkeley National Laboratory

### Title

p bar -p CROSS SECTIONS FROM 534 TO 1068 Mev

### Permalink

<https://escholarship.org/uc/item/4xz3h9nk>

### Authors

Elioff, T.  
Agnew, L.  
Chamberlain, O.  
et al.

### Publication Date

1959-07-31

UNIVERSITY OF  
CALIFORNIA  
*Ernest O. Lawrence*  
*Radiation*  
*Laboratory*

TWO-WEEK LOAN COPY

This is a Library Circulating Copy  
which may be borrowed for two weeks.  
For a personal retention copy, call  
Tech. Info. Division, Ext. 5545

BERKELEY, CALIFORNIA

UNIVERSITY OF CALIFORNIA

Lawrence Radiation Laboratory  
Berkeley, California

Contract No. W-7405-eng-48

$\bar{p}$ -p CROSS SECTIONS FROM 534 to 1068 Mev

T. Elioff, L. Agnew, O. Chamberlain, H. Steiner,  
C. Wiegand, and T. Ypsilantis

July 31, 1959

Printed for the U. S. Atomic Energy Commission

$\bar{p}$ -p CROSS SECTIONS FROM 534 to 1068 Mev

T. Elioff, L. Agnew, O. Chamberlain, H. Steiner,  
C. Wiegand, and T. Ypsilantis

Lawrence Radiation Laboratory  
University of California  
Berkeley, California

July 28, 1959

We report here measurements of the antiproton-proton, elastic, inelastic, and charge-exchange cross sections for antiproton energies of 534, 700, 816, 948, and 1068 Mev. The total cross section remains large with respect to nucleon-nucleon cross sections in the same energy range. It has not yet been possible to determine precisely what fraction of the inelastic cross section is due to annihilation.

The antiproton beam was formed in a manner similar to that of previous experiments.<sup>1, 2</sup> A schematic diagram of the experimental area is presented in Fig. 1, and Table I identifies the principal components. The 6-Bev internal proton beam of the Bevatron impinged on a carbon or polyethylene target at one of three different target positions schematically represented by T. Choice of the proper target enabled our mass spectrograph to select antiprotons within the desired energy range at angles from  $0^\circ$  to  $5^\circ$  (lab) with respect to the direction of the incident proton beam. The ratio of antiprotons to other negative particles (mostly pions) transmitted through the spectrograph was about 1/20,000 for the highest antiproton energies.

---

<sup>1</sup> Chamberlain, Segrè, Wiegand, and Ypsilantis, *Phys. Rev.* 100, 947 (1955).

<sup>2</sup> Agnew, Chamberlain, Keller, Mermod, Rogers, Steiner, and Wiegand, *Phys. Rev.* 108, 1545 (1957).

Table I

Experimental components of Fig. 1	
Symbol	Component description
T	Bevatron target area
W	Thin window of Bevatron vacuum system
C	Brass collimator 6-in. -diam by 8-in. -thick
M1, M2	60-in. -long deflection magnets with 12-by 7-in. aperture $\theta_{M1} = 17^\circ, \theta_{M2} = 25^\circ$
Q1, Q2, Q3	Sets of quadrupole focusing magnets of 8-in. aperture
S <sub>1</sub>	Plastic scintillation counter 3½ in. diam. by ¼ in thick
S <sub>2</sub>	Plastic scintillation counter 3 1/16 in. diam. by 1/4 in. thick
VSC II	Antiproton narrow-band velocity-selecting Cherenkov counter which utilizes a cyclohexane (n = 1.46, β = 0.8) radiator 3½ in. diam. and 4.7 in. long. The velocity resolution is Δβ = .03 in the range 0.95 > β > 0.70
τ	Meson Cherenkov counter which utilizes the same radiator as VSC II but views only Cherenkov light that is totally internally reflected, i. e. for β > 0.95
S <sub>3</sub>	Plastic scintillation counter 5 in. diam. by 3/8 in. thick
A	Area for H <sub>2</sub> target and final counter system

The antiprotons were distinguished from other particles in the beam by their time of flight between the scintillation counters  $S_1$ ,  $S_2$ , and  $S_3$  in coincidence with a count from the antiproton velocity-selecting Cherenkov counter, VSC II. In addition it was required that the meson Cherenkov counter,  $\bar{C}$ , did not count. The ratio of pions counted accidentally to pions transmitted through the system was less than  $10^{-7}$ .

Identified antiprotons which traversed the magnetic channel entered a target positioned immediately behind  $S_3$ . This target could be filled with either liquid hydrogen or deuterium and was completely surrounded by an array of scintillation counters. Figure 2 displays a side view of the target and counter system. Figure 3 shows the counter system from the beam-exit end. Counters  $S_4$  and  $S_5$  detected the transmitted antiprotons. The other 25 counters detected either a scattered antiproton or the products from inelastic antiproton-proton collisions. The coincidence counts between the incident antiproton and the 27 counters were displayed on an oscilloscope and photographed whenever an antiproton entered the target.

The pulses photographed on the oscilloscope film were classified as follows:

- (a) If  $S_4$  and  $S_5$  counted or if  $S_5$  counted alone, the antiproton did not interact.
- (b) Elastic scattering occurred if a single count was detected in one of the counter rings (see Fig. 3) or in counters S-1 through S-16 around the target. For scattering angles greater than  $15^\circ$  in the laboratory system, the recoil proton was also observable.
- (c) Inelastic scattering or annihilation occurred when any three or more counters registered or when two counters registered and the kinematics were not consistent with elastic scattering.

(d) A charge-exchange collision occurred when none of the counters registered.

The analysis of 70% of the film data has yielded the cross sections shown in Table II. These cross sections include small corrections for accidentals caused by neutron background in the Bevatron area, annihilations in counters, and the escape of particles through small spaces between counters. In the case of the total and the elastic cross sections, an experimental correction has been made to include forward scattering by extrapolating total cross-section measurements at small cut-off angles to zero solid angle.

Table II

$\bar{p}$ energy (Mev)	$\bar{p}$ -p Cross section (mb)			
	Total	Elastic	Inelastic	Charge exchange
534 ± 25	119 ± 6	44 ± 6	69 ± 5	6 ± 2
700 ± 33	114 ± 5	43 ± 5	64 ± 4	7 ± 2
816 ± 37	105 ± 6	37 ± 5	60 ± 5	8 ± 2
948 ± 42	96 ± 3	33 ± 3	56 ± 3	8 ± 2
1068 ± 46	96 ± 4	30 ± 3	58 ± 3	7 ± 1

Figure 4 shows the cross sections given by this experiment and, for comparison, the results of previous experiments.<sup>3, 4, 5</sup>

<sup>3</sup>Coombes, Cork, Galbraith, Lambertson, and Wenzel, Phys. Rev. 112, 1303 (1958).

<sup>4</sup>Agnew, Elioff, Fowler, Gilly, Lander, Oswald, Powell, Segre, Steiner, White, Wiegand, and Ypsilantis, Antiproton Interactions in Propane Below 200 Mev, UCRL-8822 Abstract, June 1959.

<sup>5</sup>Cork, Lambertson, Piccioni, and Wenzel, Phys. Rev. 107, 248 (1957).



In order to obtain assurance that our system could reproduce known cross sections, a positive proton beam was sent through our apparatus. This was done by scattering a 1.2-Bev internal Bevatron beam from a fourth target positioned near the region T of Fig. 1. We obtained the proton-proton cross sections at 2 energies and the results are tabulated in Table III. Precise agreement was obtained with the results of other experiments.<sup>6,7</sup>

Table III

$p^+ - p$ Cross sections for two energies			
$p^+$ energy (Mev)	$p^+ - p$ Cross sections (mb)		
	Total	Elastic	Inelastic
528	$30 \pm 7$	$24 \pm 5$	$6 \pm 3$
940	$49 \pm 5$	$26 \pm 3$	$23 \pm 3$

The new antiproton results presented here agree reasonably well with the results of a previous experiment at 457 Mev.<sup>8</sup> An apparent paradox drawn from the information of two prior experiments<sup>8,5</sup> seems to be nonexistent. The somewhat incomplete prior data (incomplete in the sense that the elastic-scattering cross section was never measured) indicated a very large absorption cross section with little or no diffraction scattering--a phenomenon that is difficult to explain.<sup>9</sup> A clarification of the situation can best be seen by the comparisons of Table IV.

<sup>6</sup>References D11, B5, and S1 in W. Hess, Summary of High-Energy Nucleon-Nucleon Cross Section Data, Revs. Modern Phys. 30, 368 (1958).

<sup>7</sup>Batson, Culwick, Clepp, and Riddiford in Proc. 1958 International Conference on High-Energy Physics at CERN (CERN, Geneva, 1958), p. 74.

<sup>8</sup>Chamberlain, Keller, Mermod, Segre, Steiner, and Ypsilantis, Phys. Rev. 108, 1593 (1957).

<sup>9</sup>Proc. 1958 International Conference on High-Energy Physics at CERN



Table IV

Comparison of $\bar{p}$ -p cross sections near 500 Mev					
Experiment	$\bar{p}$ -p Cross sections (mb)				
	Total ( $0^\circ$ )	Total ( $14^\circ$ )	Inelastic	Elastic	<del>Charge</del> exchange
Reference 8 (457 Mev)		$104 \pm 8$	$89 \pm 7$	-	-
Reference 5 (500 Mev)	$97 \pm 4$	-	-	-	-
This experiment (534 Mev)	$119 \pm 6$	$93 \pm 6$	$69 \pm 5$	$44 \pm 6$	$6 \pm 2$

From the 534-Mev data, one observes that more than half of the scattering is strongly peaked forward within a  $14^\circ$  laboratory angle. The latest results also indicate that the total elastic-scattering cross section constitutes  $\sim 1/3$  of the total cross section in the energy range we have measured. This ratio has been indicated by a phenomenological black-sphere model of Koba and Takeda for a sphere radius of  $\sim 2/3 \hbar/m_\pi c$ .<sup>10</sup>

It is surprising that the inelastic cross section does not decrease appreciably with increasing energy which may indicate a longer-range annihilation interaction than expected.<sup>9</sup> The Ball-Chew theory,<sup>11</sup> which is in agreement with the low-energy antiproton data, attributes the annihilation interaction to a rather short-range absorbing core. Of course the inelastic

<sup>10</sup>Z. Koba and G. Takeda, Progr. Theoret. Phys. (Kyoto) 19, 269 (1958).

<sup>11</sup>J. Ball and G. Chew, Phys. Rev. 109, 1395 (1958).

cross section as presented here includes both annihilation and meson production. From the partial analysis of the 948-Mev inelastic events, it appears that not more than about 10 mb of the inelastic cross section can be due to meson production. (The remaining 46 mb must then be attributed to annihilation.) This analysis is based on the assumption that production of 2 or more mesons is negligible except in annihilation. The assumption seems warranted because double meson production is known to be very small in nucleon-nucleon collisions at this energy.<sup>7, 12, 13</sup>

Upon completion of our analysis we hope to more fully discuss the inelastic process. In addition to the antiproton-proton cross sections, we have the antiproton-deuteron cross sections at the same five energies. These results will be presented in a later publication.

#### Acknowledgments

We are grateful to Professor Emilio Segrè for his interest and advice during the critical stages of the experiment. We thank Drs. Richard Lander, Norman Booth, and Jan Button for their help during the course of the experiment.

---

<sup>12</sup>Fowler, Shutt, Thorndike, Whittemore, Cocconi, Hart, Block, Harth, Fowler, Garrison, and Morris, Phys. Rev. 103, 1493 (1956).

<sup>13</sup>W. A. Wallenmeyer, Phys. Rev. 105, 1058 (1957).

FIGURE LEGENDS

- Fig. 1. Schematic view of the Bevatron experimental area. See Table I.
- Fig. 2. Side view of target and counter system. For clarity, the figure is not shown precisely to scale. The container (A) which could be filled with liquid hydrogen or deuterium is a stainless steel cylinder 12 in. long and 6 in. in diameter with 0.008-in. walls except for the beam entrance wall which is 0.010-in. mylar. Sixteen scintillation counters, S-1 through S-16 cylindrically surround the container (A). Each has dimensions 38 by 4.1 by 0.375 in. Scintillators  $S_E$ , A, B, C, D,  $\alpha$ ,  $\beta$ ,  $\gamma$ ,  $\delta$ ,  $S_4$ , and  $S_5$  are shown more explicitly in the next figure. The lead between the target and the scintillators is removable. The heat shield (C) is 0.003-in. copper; (E) is a thin region of the vacuum wall which is 0.035-in. aluminum.
- Fig. 3. Schematic view from the beam-exit end of the counter system, which displays counters A, B, C, D,  $\alpha$ ,  $\beta$ ,  $\gamma$ ,  $\delta$ ,  $S_4$ , and  $S_5$  and their overlapping regions as well as an end view of counters S-1 through S-16.
- Fig. 4. Antiproton-proton total, elastic, inelastic, and charge-exchange cross sections as a function of antiproton laboratory kinetic energy. The round points are the results of this experiment. The triangular points are from reference 5 and reference 3. The square points are from reference 4. For clarity the inelastic points are darkened.

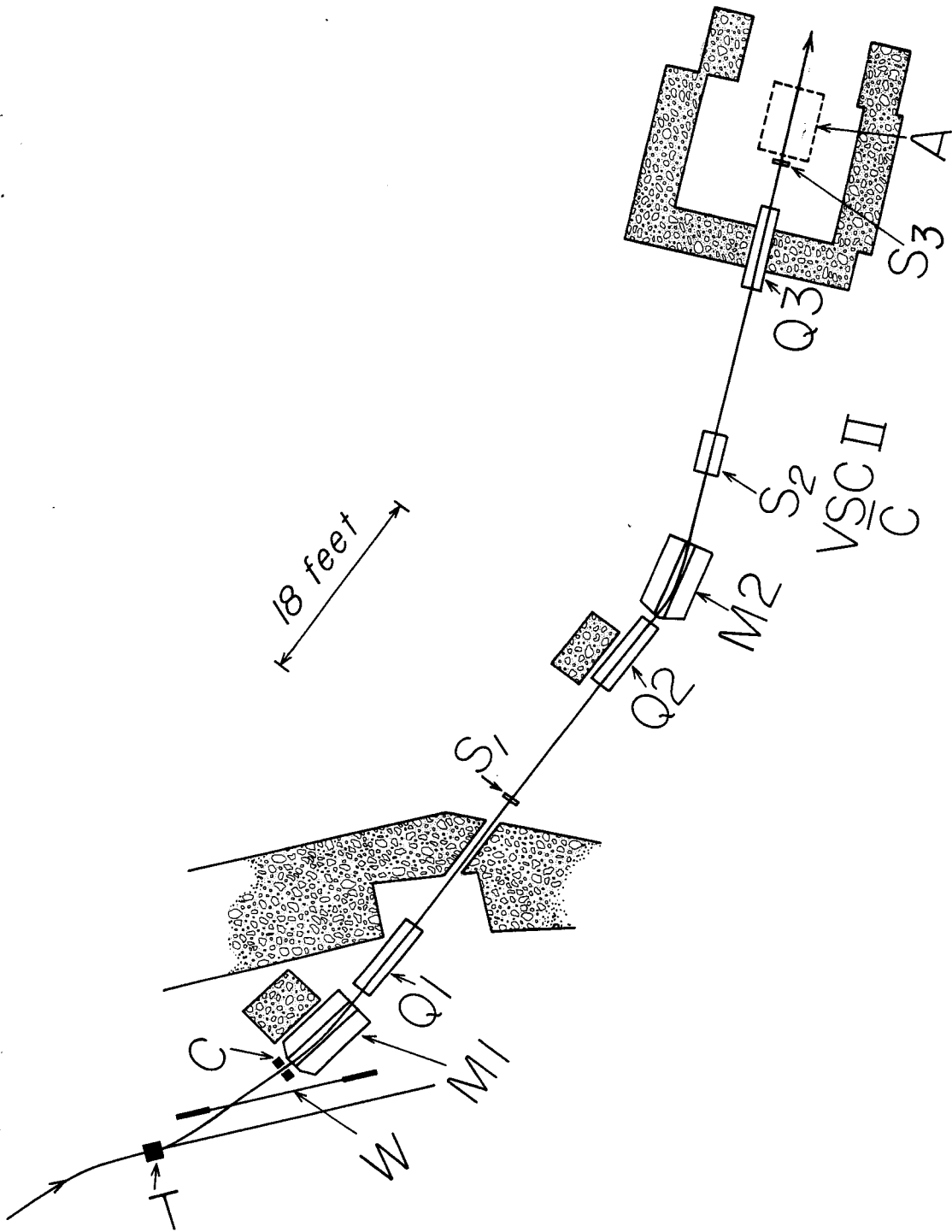
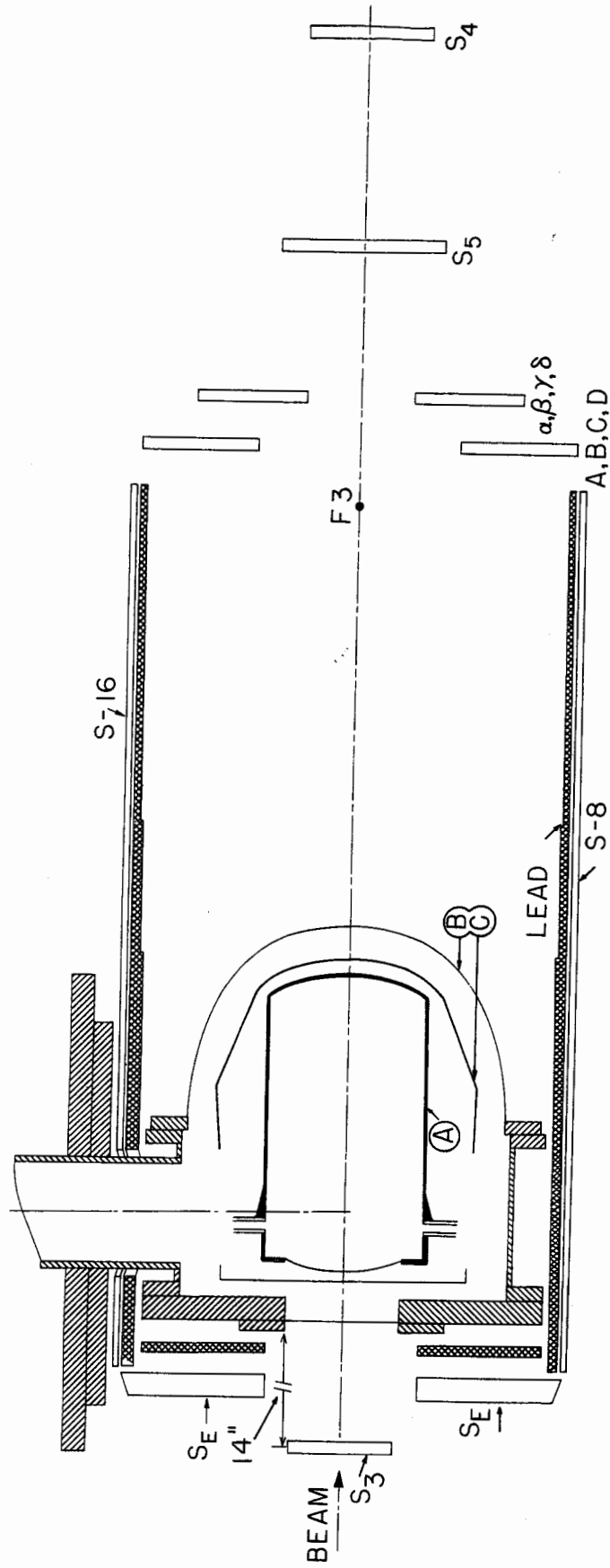


Fig. 1



MUB-286

Fig. 2

